Mineralium Deposita (2005) 40: 218–230
DOI 10.1007/s00126-005-0478-8

ARTICLE

Chusi Li · Edward M. Ripley

Empirical equations to predict the sulfur content of mafic magmas at sulfide saturation and applications to magmatic sulfide deposits

Received: 3 September 2004 / Accepted: 1 April 2005 / Published online: 21 June 2005

Abstract Empirical equations to predict the sulfur content of a mafic magma at the time of sulfide saturation have been developed based on several sets of published experimental data. The S content at sulfide saturation (SCSS) can be expressed as:

$$\ln X_S = 1.229 - 0.74(10^4/T) - 0.021(P) - 0.311 \ln X_{FeO} - 6.166X_{SiO_2} - 9.153X_{Na_2O} + K_2O - 1.914X_{MgO} + 6.594X_{FeO}$$

where T is in degrees Kelvin, X is mole fraction and P is in kbar. The squared multiple correlation coefficient (r^2) for the equation is 0.88. Application of the equation to data from sulfide-saturated mid-ocean ridge basalts (MORB) samples show that the SCSS is closely predicted for primitive MORBs, but that accuracy decreases for lower T (<1,130°C) and more evolved MORB samples. This suggests that because the calibrations are based on anhydrous experimental runs done at temperatures of 1,200°C and above, it is not possible to extrapolate them to significantly lower temperatures and hydrous conditions. Because the SCSS of a primitive MORB magma increases with decreasing P, sulfide saturation in MORB appears to be a function of the degree of en route assimilation of S from country rocks as well as the degree of fractional crystallization in shallow staging chambers. Application of the equation to the high-Timpact melt sheet that produced the Sudbury Igneous Complex and associated Ni–Cu sulfide ores indicates that sulfide-saturation was reached at ~1,500°C, well above the start of orthopyroxene crystallization at ~1,190°C. This would permit ample time for the gravitational settling and collection of immiscible sulfide liquid that produced the high-grade ore bodies. The development of a platinum group element (PGE)-enriched layer in the Sonju Lake Intrusion of the Duluth Complex is thought to be due to the attainment of sulfide saturation in the magma after a period of fractional crystallization. Using the composition of the parent magma of the Sonju Lake Intrusion the presented equation indicates that sulfide saturation would have been reached at ~60% crystallization, when iron oxide was a liquidus mineral; the prediction is in agreement with field evidence which indicates that PGE-enrichment occurs in the oxide-rich gabbro zone. Contamination and mixing processes that may be related to the attainment of sulfide saturation in mafic magmas can also be evaluated. Mixing of a siliceous melt and a liquid of olivine tholeiite composition, similar to that thought to be a reasonable parental composition for many Duluth Complex intrusions, can induce sulfide saturation at mixing ratios in excess of ~0.1. If the contaminant contains low quantities of sulfur the mixing ratio required to promote saturation is reduced. Mixing of mafic magmas at various stages of fractionation is evaluated using magma compositions that are thought to be appropriate for the generation of the Merensky Reef in the Bushveld Complex. Magma mixing is shown to be an effective process for the attainment of sulfide saturation, depending strongly on the sulfur concentrations of the end-member magmas.

Keywords Sulfur · Solubility · Magmatic sulfide deposits · Nickel · PGE

C. Li (✉) · E. M. Ripley
Department of Geological Sciences,
Indiana University, Bloomington,
IN 47405, USA
E-mail: cli@indiana.edu
Tel.: +1-812-855-1196
Fax: +1-812-855-7961

Introduction

Several well-constrained experimental studies have now been undertaken that address the solubility of sulfur in magmas. Sulfur is a key element in many geological processes, including core–mantle differentiation, sulfide ore genesis, and volcanic degassing. For many processes, especially those associated with ore genesis, the prime

factor is the point at which an immiscible sulfide liquid will separate from a magma, or a solid sulfide mineral will crystallize. Shima and Naldrett (1995) have referred to this value as the S content at sulfide saturation (SCSS), whereas Holzheid and Grove (2002) have referred to this value as the S solubility limit. Although there is now a general consensus regarding the major controls on S solubility in magmas, the prediction of the S solubility limit remains difficult without knowledge of several intensive parameters, as well as melt composition. In this paper we review existing experimental data and appropriate discussions that pertain to the solution of S in mafic magmas, and the prediction of the S content of a magma at the time of sulfide liquation. We present an empirical expression that predicts the available experimental data on the limit of S solubility to ~10%, as a function of temperature, pressure, and melt composition.

Background

The solution of S in silicate melts was discussed by Fincham and Richardson (1954) in terms of reaction between base metal oxides and either S^{2-} or SO_4^{2-}. They proposed that for silicate melts at Po_2 less than $\sim 10^{-3}$ atm, sulfur concentration was controlled by the general equilibrium:

$$S_{(melt)} \text{ or } S^{2-} + \frac{1}{2}O_2 = O_{(melt)} \text{ or } O^{2-} + \frac{1}{2}S_2. \quad (1)$$

Because free oxygen is unlikely to be present in a melt (e.g., Hess 1980), and because experimental studies (e.g., Haughton et al. 1974; O'Neill and Mavrogenes 2002) have shown that FeO is an extremely important component in controlling S solubility, the solution reaction is commonly presented as:

$$FeO_{(sil)} + \frac{1}{2}S_2 = FeS_{(sil)} + \frac{1}{2}O_2. \quad (2)$$

At sulfide saturation an immiscible sulfide liquid may form and this relationship can be paired with $FeS_{(sil)} \rightleftharpoons FeS_{(sulf)}$ to yield the heterogeneous equilibrium:

$$FeO_{(sil)} + \frac{1}{2}S_2 = FeS_{(sulf)} + \frac{1}{2}O_2. \quad (3)$$

An evaluation of reaction (3) suggests that T (which affects ln K), log fO_2, log fS_2, and melt composition (e.g., X_{FeO}) will be important variables controlling sulfide dissolution. These variables were highlighted in the 1-atm study of Haughton et al. (1974), who fit an equation to describe the S content of their charges in terms of melt composition. Experimental 1-atm studies by Danckwerth et al. (1979) were done using high-TiO_2 mare basalts, but showed the importance of the same variables on S solubility. O'Neill and Mavrogenes (2002) confirmed that temperature, melt composition, and fO_2/fS_2 were major controls of S dissolution in melts at 1 atm pressure. They emphasized the overwhelming control that Fe content has on S solubility in magmas, and related the concept of sulfide capacity initially presented by Fincham and Richardson (1954), i.e., $C_{\{S} = (S)\cdot(fO_2/fS_2)^{1/2}$, to the S content of the silicate melt at sulfide saturation (see Appendix). They noted that relating expressions for C_S and the equilibrium constant for (3) results in a solution for SCSS that is independent of fS_2 and fO_2. O'Neill and Mavrogenes (2002) also state that the SCSS is dependent on the activities of FeS and FeO, which will be affected by variations in fO_2/fS_2.

Figure 1 contains plots based on sulfide-saturated runs presented by Haughton et al. (1974), Danckwerth et al. (1979), and O'Neill and Mavrogenes (2002). The experimental/analytical uncertainty for ln X_s in these plots is taken from reported literature values. The uncertainties in the ln(fS_2/fO_2) and ln X_{FeO} values are generally within the utilized symbols. The data of Haughton et al. (1974) and Danckwerth et al. (1979) show positive relationships between ln X_S and ln (fS_2/fO_2). The data from O'Neill and Mavrogenes (2002) show much less variation in ln $X_S$with the fS_2/fO_2 ratio, but illustrate the clear compositional dependency of ln X_S. The PAL-synthetic tholeiite and olivine tholeiite compositions of O'Neill and Mavrogenes (2002) show an increase in ln X_S at higher ln(fS_2/fO_2) values, similar to the data of Haughton et al. (1974) and Danckwerth et al. (1979). What is important is that there is a measure of consistency between the experiments (see restrictions for the data from Haughton et al. (1974) given in Fig. 1 caption), and that the effect of melt composition on the SCSS is clearly shown. Wallace and Carmichael (1992) used the data of Haughton et al. (1974) to derive an empirical expression for sulfide solubility in mafic magmas in terms of temperature, log fO_2, log fS_2, and melt composition. Li and Naldrett (1993) also presented an algorithm for computing the amount of S that dissolves in a mafic magma as FeS as a function of temperature, a_{FeO}, fS_2, and fO_2.

Another interesting relationship shown by all of the experiments is illustrated in a ln X_s–ln X_{FeO} plot (Fig. 1b). All of the data show a steep positive relationship at ln X_{FeO} values in excess of approximately −2.5. The plot shows that for all starting melt compositions the trends tend to flatten, and perhaps show an upturn at low FeO contents. Because of the importance of water in low-FeO magmas, these low-X_{FeO} runs are not particularly relevant geologically. However, the leveling out of the ln X_s values after showing a steep slope at high ln X_{FeO} values has been interpreted from two different approaches. O'Neill and Mavrogenes (2002) show that the SCSS may strongly depend on X_{FeO} values at high-FeO contents, but that at lower FeO values a negative dependency between S and FeO is due to control by r_{FeO}, which has a negative sign in the expression for SCSS. Poulson and Ohmoto (1990) interpret the trend as a function of solution mechanism and suggest that the slope of ~2 at high X_{FeO} values is produced via a reaction such as:

$$2FeO_{(melt)} + FeS_{(melt)} = 2FeO \cdot FeS_{(melt)}. \quad (4)$$

Poulson and Ohmoto (1990) proposed another solution mechanism for the flat portion of the plot, following a reaction of the form:

$$FeS_{(sil)} = FeS_{(sulf)}. \quad (5)$$

The Poulson and Ohmoto (1990) solution mechanism at elevated X_{FeO} values is attractive, as it offers a concrete reason for the increase in the SCSS with FeO content of the silicate melt. For example, why an increase in the FeO content of a silicate magma saturated with FeS (and with buffered fS_2 and fO_2) should cause additional sulfide dissolution is not intuitively obvious. However, the formation of an FeO–FeS complex dictates that sulfide would dissolve, and the saturation limit must increase. Whether the solution mechanism represented by Eq. 4 is correct or not remains an uncertainty, but it does highlight the probable importance of oxygen in sulfur dissolution. The highly non-ideal nature of immiscible Fe–S–O liquids has been highlighted by Kress (1997, 2000), and this non-ideality may be responsible for the observed relationships between S and Fe concentrations.

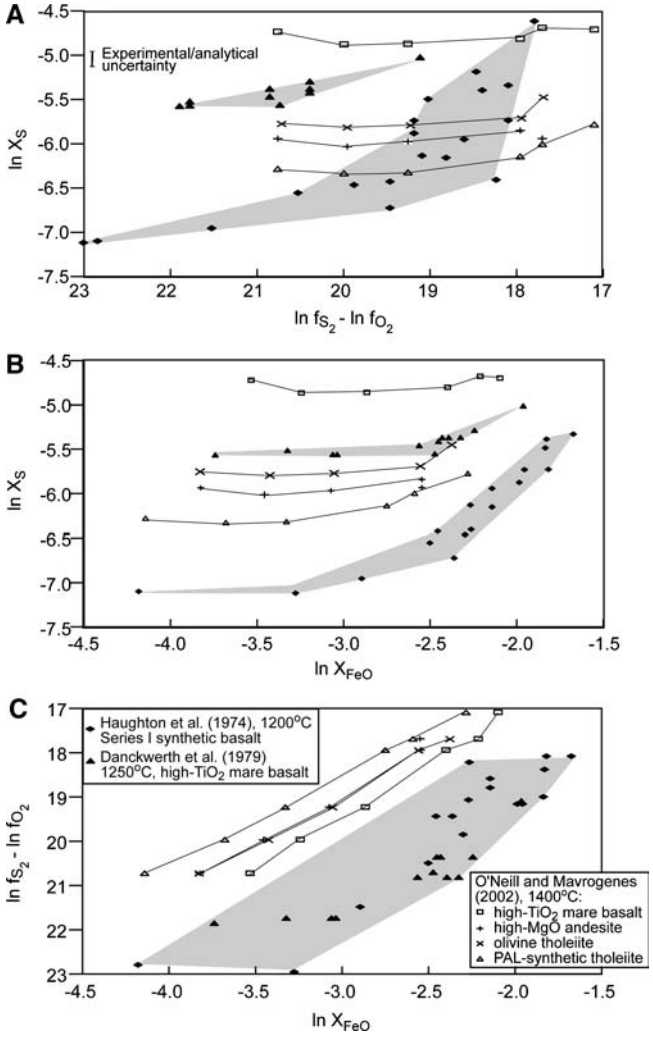

Fig. 1 One-atmosphere data for sulfide-saturated samples from Haughton et al. (1974), Danckwerth et al. (1979), and O'Neill and Mavrogenes (2002): **a** ln X_S –ln(fS_2/fO_2), **b** ln X_S –ln X_{FeO}, and **c** ln(fS_2/fO_2) –ln X_{FeO}. One-atmosphere data for Series I sulfide-saturated samples from Haughton et al. (1974) were utilized, with the following restrictions. For duplicate runs, samples with the lowest FeO content in the silicate liquid were chosen. This is based on the premise that samples with the lowest FeO (sil) would have more FeS (sulfide liquid), and would record a closer approach to equilibrium. Series II data of Haughton et al. (1974) were shown by O'Neill and Mavrogenes (2002) not to record equilibrium, and have been excluded in our analysis. The same is true for samples from Buchanan and Nolan (1979). For clarity the average MORB and DB/3-synthetic tholeiite runs of O'Neill and Mavrogenes (2002) are not shown, but they are similar to olivine tholeiite

Figure 1c shows the positive relationship between ln X_{FeO} and ln(fS_2/fO_2) observed in the experiments. The offsets in the trends are attributable to the effects of both melt composition and temperature [1,200–1,250°C for Haughton et al. (1974) and Danckwerth et al. (1979) and 1,400°C for O'Neill and Mavrogenes (2002)]. The ln(fS_2/fO_2) ratio of the sulfide-saturated mafic melts can be predicted based on melt composition and temperature to be within ±5% (Fig. 2) using the following equation:

$$\ln(fS_2/fO_2) = a + b(10^4/T) + c\ln X_{FeO} + \sum d_i X_i. \quad (6)$$

where T is in degrees Kelvin, $X_{FeO}$is the mole fraction of FeO in the silicate melt and a, b, c, and d_i are constants determined from the results of sulfide-saturated experimental runs (Table 1). The summation is over the number of silicate melt components, " i".

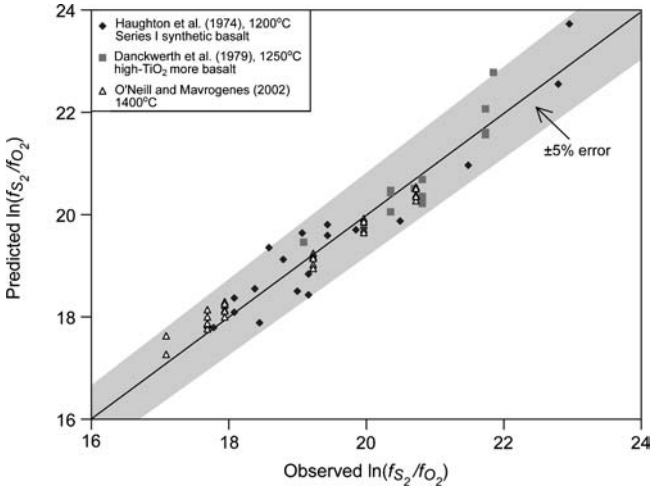

Fig. 2 Predicted vs observed ln(fS_2/fO_2) in silicate melts for sulfide-saturated experimental runs performed at 1 atm. The equation has been generated by forward stepwise linear regression and yields an r^2 value of 0.94. Although ln X_S was considered as a variable its coefficient was too low to be significant. The plot illustrates the strong relationship between fO_2/fS_2, melt composition, and temperature

Table 1 Best fit parameters for Eq. 6

Coefficient	Value	Standard error
a	−6.470	2.352
b	3.864	0.316
c	−1.574	0.174
$d\,SiO_2$	−3.544	0.854
$d\,Na_2O + K_2O$	−38.752	7.598
$d\,FeO$	−6.510	2.770

Prediction of the sulfur content of a mafic magma at sulfide saturation

One-atmosphere

Despite the different approaches taken in describing S solubility and the SCSS in a mafic magma, the experimental data summarized in Figs. 1 and 2 provide an exceptional framework for an empirical evaluation of the SCSS. O'Neill and Mavrogenes (2002) present an equation (their equation 27) for SCSS at 1 atm that depends on ln K for Eq. 3, melt composition, and γ_{Fe}. We have derived an expression using forward stepwise linear regression that relates the SCSS to temperature and melt composition as follows:

$$lnX_S = a + b(10^4/T) + c\ln X_{FeO} + \sum d_i X_i, \qquad (7)$$

where the coefficients and variables are as described for Eq. 6 and are given in Table 2. An r^2 (squared multiple correlation coefficient) value of 0.95 is returned from the regression (Fig. 3). This expression does not explicitly involve either fO_2 or fS_2. The reason for this is that at sulfide saturation the fS_2/fO_2 ratio of the melt can be expressed as a function of melt-composition and temperature (Fig. 2), in agreement with the compositional dependency of the C_S value reviewed by O'Neill and Mavrogenes (2002).

Variable pressures

The effect of pressure on S solubility in mafic magmas has been shown to be significant. Experimental studies by Mavrogenes and O'Neill (1999) and Holzheid and Grove (2002) confirmed earlier results by Helz (1977), Huang and Williams (1980), and Wendlandt (1982) for anhydrous compositions, which showed an inverse relationship between pressure and the SCSS. The results of these studies differ from those of Mysen and Popp (1980) for $CaMgSi_2O_6$ and $NaAlSi_3O_8$ melts where a positive pressure dependency for the SCSS was determined. Although considerable amounts of speculation have been offered to explain the discrepancies between the studies, no definitive reasons have emerged.

Table 2 Best fit parameters for Eq. 7

Coefficient	Value	Standard error
a	2.181	0.552
b	−1.234	0.056
c	−0.427	0.061
$d\,SiO_2$	−4.280	0.567
$d\,TiO_2$	3.198	0.842
$d\,FeO$	11.223	1.031

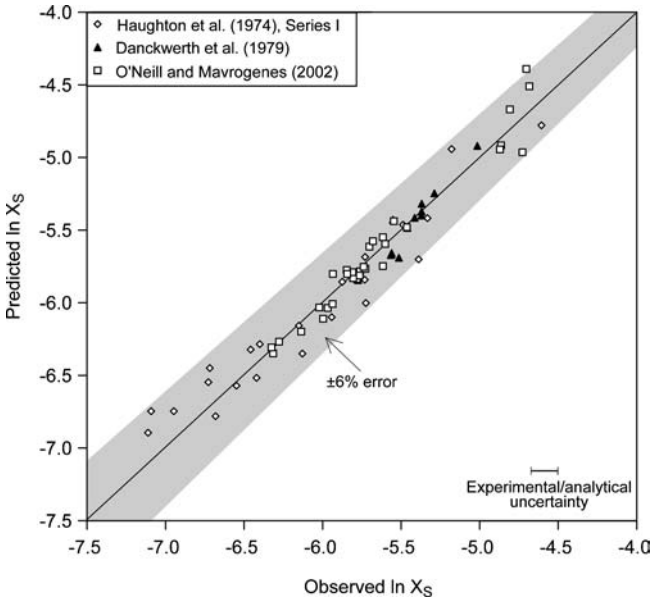

Fig. 3 Predicted vs observed ln X_S in silicate melts for sulfide-saturated experimental runs performed at 1 atm

Mavrogenes and O'Neill (1999) fit their experimental results at variable pressures to the following equation:

$$\ln S(\text{ppm}) = A/T + B + C(P/T) + \ln a_{FeS}^{sulfide}. \qquad (8)$$

Holzheid and Grove (2002) also present an equation for predicting the SCSS at variable pressures. They modified the Mavrogenes and O'Neill (1999) equation by adding a term that evaluates the ratio of non-bridging oxygens to tetrahedrally coordinated cations and takes into account the effect of melt polymerization on S solubility.

Equation 7 can be modified to describe the SCSS at variable pressures by adding a pressure term:

$$\ln X_S = a + b(10^4/T) + cP + d\ln X_{FeO}^{sil} + \Sigma e_i X_i, \qquad (9)$$

where P is in kilobars and regression coefficients a–e are as listed in Table 3. Equation 9 can be calibrated using the experiments of sulfide-saturated systems performed at high pressures by Mavrogenes and O'Neill (1999), Holzheid and Grove (2002), and Jugo et al. (2005) (Table 3). The silicate liquid compositions of Wendlandt (1982) are not reported (although presumably were international standards), and the results of Li and Agee (1996, 2001) must be treated separately because the sulfide liquids of their experiments contained significant amounts of Ni (8–17 wt%). The experiments of Holzheid and Grove (2002) also contain variable amounts of

Table 3 Best fit parameters for Eq. 9

Coefficient	Value	Standard error
a	1.229	0.537
b	−0.740	0.054
c	−0.021	0.002
d	−0.311	0.093
$e\mathrm{SiO_2}$	−6.166	0.412
$e(\mathrm{Na_2O}+\mathrm{K_2O})$	−9.153	1.440
$e\mathrm{MgO}$	−1.914	0.459
$e\mathrm{FeO}$	6.594	1.116

Ni and Co. We have excluded runs where the sulfide liquid contained in excess of 1 wt% (Ni + Co), and also the experiments of Mavrogenes and O'Neill (1999) where the computed $a_{\mathrm{FeS}}^{\mathrm{sulfide}}$ was ~0.5. A total of 45 experimental results at high pressures (17 from Mavrogenes and O'Neill 1999; 15 from Holzheid and Grove 2002; 13 from Jugo et al. 2005), along with the 66 runs done at atmospheric pressure, were used to calibrate Eq. 9 using forward stepwise linear regression analysis. The squared multiple correlation coefficient (r^2) of the samples is 0.88. The ranges of pressure, temperature, and melt compositions of the samples used for calibration are listed in Table 4. The predicted and observed ln X_{S} values are compared in Fig. 4. The error of prediction from Eq. 9 is less than 10%.

Sulfur bonding with cations other than iron

The importance of Fe–S–O bonding appears to overshadow other possible combinations in Fe-rich basaltic melts. However, the relatively high values for S solubility in Fe-poor melts (e.g., values in excess of 1,000 ppm: Fincham and Richardson 1954; Carroll and Rutherford 1985; Bradbury 1983), strongly indicates that bonding of S with other cations is feasible. In high-$f\mathrm{O_2}$ magmas, Carroll and Rutherford (1985) proposed $\mathrm{Ca^{2+}}$–$\mathrm{SO_4^{2-}}$ complexing to explain high S contents that accompany anhydrite saturation. However, dissolved S values may also exceed 1,000 ppm in Fe-poor melts at low $f\mathrm{O_2}$ values (Fincham and Richardson 1954; O'Neill and Mavrogenes 2002), which suggests that complexing agents other than $\mathrm{Fe^{2+}}$ must also be involved.

Chalcophile elements such as Ni, Cu, and Co partition strongly into an immiscible sulfide liquid (e.g., Peach et al. 1990; Gaetani and Grove 1997; Li et al. 2003a, b), which will affect the a_{FeS} in the sulfide liquid. Accordingly, the SCSS is expected to vary in response to the concentration of chalcophile elements in a silicate

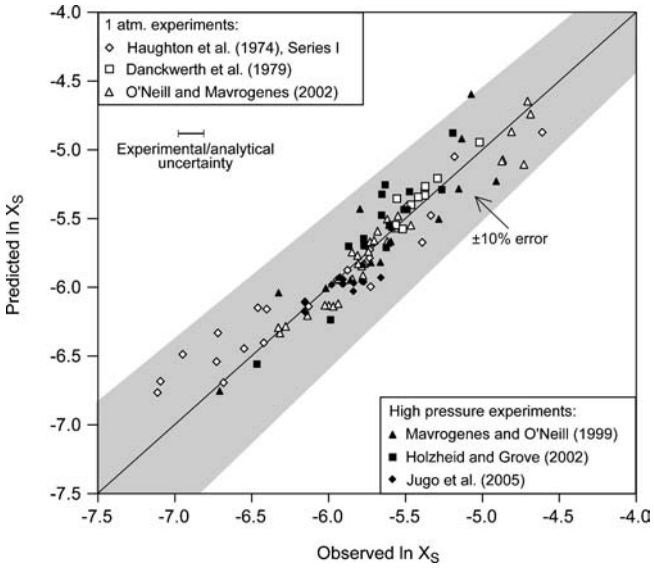

Fig. 4 Predicted vs observed ln X_{S} for silicate melts of sulfide-saturated experiments using synthetic basalts of 1 bar to 90 kbar

magma. Figure 5 compares the predicted and measured values of the SCSS for high-pressure silicate liquids that coexist with sulfide liquids that contain from 8 to 17 wt% Ni (Li and Agee 1996, 2001) and (Ni + Co) from 5 to 9 wt% (Holzheid and Grove 2002). The measured S contents in the silicate melts of Li and Agee (1996, 2001) are up to 20% higher or lower than the predicted values; these data are difficult to interpret and provide no clear insight into the effect of Ni on S solubility limits. The measured S concentrations in the silicate melts of Holzheid and Grove (2002) agree well with predicted values for the SCSS, and suggest that at least for these compositions the effect of 5–9 wt% (Ni + Co) on the S solubility limit is not large. Data from Ripley et al. (2002a) clearly illustrate the effects of the composition of the sulfide liquid on the S content of a coexisting basaltic silicate glass. A systematic decrease in observed ln X_{S} values relative to predicted ln X_{S} values correlates with an increase in Cu content of the sulfide liquid from 9 to 77 wt% (Fig. 5). Samples with Cu concentrations in the sulfide liquid less than ~12 wt% Cu fall within 4% of the values calculated from Eq. 9. The systematic decrease in observed ln X_{S} values is in accord with the decrease in the a_{FeS} of the sulfide liquid.

Of particular importance for $\mathrm{H_2O}$-bearing magmas is the potential role of $\mathrm{H_2}$–S bonding. Burnham (1979) proposed that S may dissolve in hydrous magmas as $\mathrm{HS^-}$ in a manner analogous to at least some $\mathrm{H_2O}$ (as $\mathrm{OH^-}$). Bradbury (1983) demonstrated that the S content in hydrous albite melt (values up to 2,000 ppm)

Table 4 Ranges of experimental P, T, and silicate melt composition (wt%) used for the calibration of Eq. 9

	P	T(°C)	$\mathrm{SiO_2}$	$\mathrm{TiO_2}$	$\mathrm{Al_2O_3}$	$\mathrm{Cr_2O_3}$	$\mathrm{Fe_2O_3}$	FeO	MnO	MgO	CaO	$\mathrm{Na_2O}$	$\mathrm{K_2O}$
Range	1 b–90 kbar	1,200–1,800°C	38.9–67.6	0–15.3	6.9–22.8	0–1	0–2.23	0.8–25.7	0–0.3	3.1–22.6	6.0–17.1	0–6.4	0–1.6

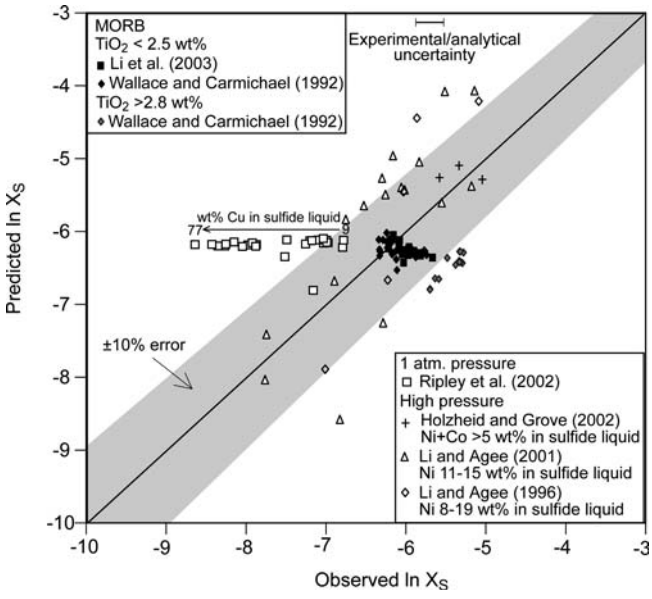

Fig. 5 Comparison of observed vs predicted ln X_s in silicate melts of various sulfide-saturated systems. The predicted ln X_S values were obtained from Eq. 9. The high-pressure samples of Li and Agee (1996, 2001) contain high concentrations of Ni in the sulfide liquid and show departures of up to 20% from the predicted values. The MORB samples from Wallace and Carmichael (1992) and Li et al. (2003a) which do not fall in the *shaded interval* are evolved, some with up to 3.75 wt% TiO_2

increased with increasing activity of H_2S and pressure, and decreased with increasing Fe content of the melt. Caroll and Rutherford (1985) also showed that S solubility increased with pressure in hydrous, dacitic magma. Bradbury (1983) proposed the following reaction to explain the dissolution of pyrrhotite in hydrous $NaAlSi_3O_8$ melt:

$$FeS_{(po)} + O^{2-}(m) + H_2O(v) = FeO(m) + SH^-(m) + OH^-(m). \quad (10)$$

A similar reaction for melt species may be:

$$FeS \cdot FeO(m) + O^{2-}(m) + H_2O(m) = 2FeO(m) + SH^-(m) + OH^-(m) \quad (11)$$

Gorbachev and Kashiceva (1986) performed a series of experiments on basaltic to picritic melts in equilibrium with a sulfide liquid and either an H–O–S or H–O–C–S vapor at temperatures of 1,250 and 1,350°C. They found that at each temperature the SCSS for the silicate melts increased slightly with increasing P up to 15 kbar, but decreased progressively with P above this value. The reasons for the changes in the SCSS with Pin their experiments are unknown, but it is clear that additional experiments that address the SCSS for hydrous, basaltic magmas are needed. The lower pressure results for hydrous magmas are opposite to the high-pressure results for anhydrous basaltic systems discussed above. Deciphering the systematics of S solubility and P variations in both hydrous and anhydrous mafic to intermediate magmas is essential for evaluations of S degassing phenomenon and sulfide ore genesis.

Experimental values for SCSS compared to data from sulfide-saturated seafloor basalts

Another method for evaluating the SCSS is to utilize natural samples that represent quenched basaltic liquids. The common presence of immiscible sulfide globules in mid-ocean ridge basalts (MORB) indicates that these basaltic liquids are saturated or nearly saturated with sulfide liquid at the time of eruption (Mathez 1976; Wallace and Carmichael 1992). Mathez (1976) suggests that pillow lavas that erupt at ocean depths in excess of ~2,000 m have not undergone extensive degassing and that quenched pillow rinds preserve near-liquidus phase relations. For this reason quenched submarine glasses are the best natural samples available for the study of equilibria in sulfide-saturated basaltic liquids.

Wallace and Carmichael (1992) analyzed 61 basaltic glasses from both spreading centers and seamounts for their major element compositions, S contents, temperature, fO_2, and fS_2. Forty-four of those samples were collected from water depths greater than 2,000 m and are not thought to have undergone significant degassing. The major element compositions of these samples are not listed in Wallace and Carmichael (1992), but were obtained upon request from the authors and are tabulated in Li et al. (2001a).

Of particular significance is a comparison of experimental results with data from the natural samples. Figure 5 illustrates that Eq. 9, based on experimental results, accurately predicts the SCSS for primitive MORB liquids, but does not predict the SCSS for evolved MORB liquids. The evolved liquids are characterized by high TiO_2 (>2.8 wt%), high FeO (>14 wt%), low temperature (<1,130°C), and up to 1 wt% H_2O (Wallace and Carmichael 1992; Li et al. 2003a). Experimental data are not available at temperatures less than 1,200°C, and extrapolation to the low T and hydrous conditions of the evolved MORB glasses is thought to be the primary reason for the discrepancy.

The experimental data on the SCSS have important ramifications with respect to the interpretation of sulfide-saturated MORB magmas. Lesher and Stone (1996) estimated a depleted mantle S concentration in the range of 150–215 ppm. Melting from 10% to 20% (Langmuir et al. 1992) will produce a MORB liquid with ~1,000–2,000 ppm S. The experimental results of Mavrogenes and O'Neill (1999) and Holzheid and Grove (2002) show that such a melt should be saturated in sulfide. Figure 6 illustrates the change of the SCSS with pressure predicted from Eq. 9. The plot indicates that a MORB liquid that is sulfide-saturated at its source will not be so when it reaches the surface (Fig. 6). Both Mavrogenes and O'Neill (1999) and Holzheid and Grove (2002) have emphasized that a mantle-derived mafic magma should arrive at the surface sulfide-saturated only if the magma

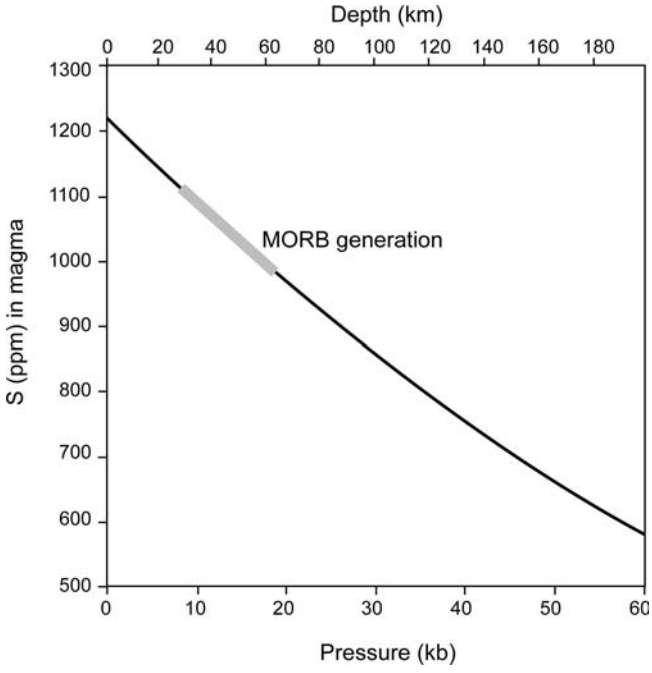

Fig. 6 The SCSS vs depth (pressure) for a mid-ocean ridge basalt, sample K-17-20, Galapagos 95.5°W (Table 5, from Wallace and Carmichael 1992). The temperature of the magma when it reaches the surface is 1,200°C according to MELTS (Ghiorso and Sack 1995), and the adiabatic gradient is assumed to be 3°C/kbar. The ratios of FeO/Fe_2O_3 have been adjusted to correspond to log fO_2 of QFM-2. The depth for the initial generation of a primitive MORB liquid is from Green et al. (1979) and Presnall et al. (2002)

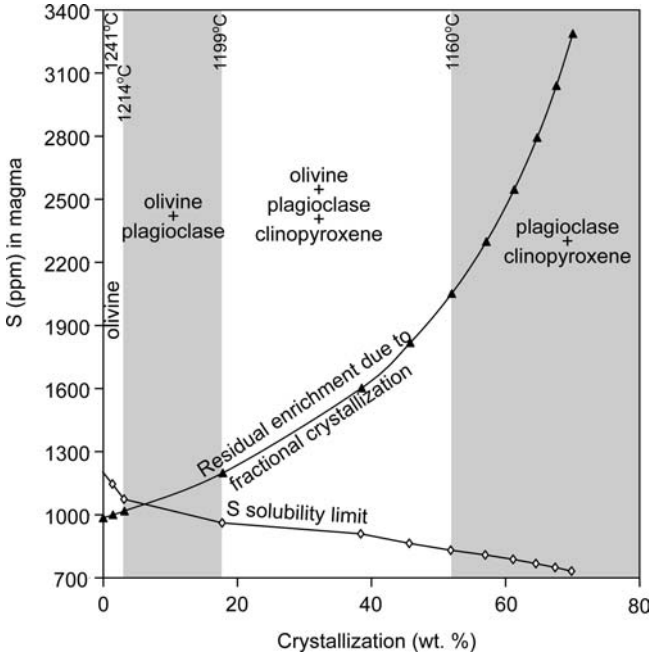

Fig. 7 Comparison of the SCSS with residual S enrichment during fractional crystallization for a primitive MORB (sample K-17-20 from Galapages 95.5°W, Wallace and Carmichael 1992). Fractional crystallization is simulated assuming 0.2 wt% H_2O in the initial liquid, QFM-1, 1 kbar, and 1°C increments using MELTS (Ghiorso and Sack 1995). The SCSS in the silicate melt is calculated from Eq. 9

had undergone extensive fractional crystallization or if assimilation of country rock S occurred en route to the surface.

The data from seafloor basalt glasses (Wallace and Carmichael 1992; Mathez 1976; Li et al. 2003a) supply strong evidence for the importance of these processes. As noted above, at its source a MORB liquid is expected to contain ~1,000–2,000 ppm S. The experimental data indicate that approximately one half of this amount could be present as immiscible sulfide liquid (Fig. 6). Entrainment of immiscible sulfide droplets into a rising MORB magma might be envisioned as a means to generate at low pressure a magma that is just saturated with sulfide and contains ~1,000 ppm dissolved S. That such a process does not occur is strongly suggested by the platinum group element (PGE) contents of most MORB. Crockett (1979, 2002) summarized the PGE data from mafic and ultramafic rocks, and emphasized that the strongly depleted nature of MORB indicates that PGEs were collected by sulfide liquids that remained at depth. In order for seafloor basalts to erupt with sulfide globules present, assimilation of S from the oceanic crust must occur en route to the surface, and/or fractional crystallization must occur in shallow staging chambers. Layered gabbros in the oceanic crust are known to contain sulfide minerals (e.g., Alt 1994), and selected assimilation of S from this source could bring the S contents of primitive MORB liquids to those required to achieve sulfide saturation.

The data of Wallace and Carmichael (1992) and Li et al. (2003a) also illustrate the effects of fractional crystallization on S contents and saturation of residual basaltic liquids. Figure 7 illustrates the increase in S content of residual liquids due to fractional crystallization, and observed SCSS of MORB (Table 5). Less than 10% of crystalllization is required to induce sulfide saturation in a MORB liquid. The S contents of a basaltic liquid produced as a result of fractional crystallization far exceeds those required to achieve sulfide saturation. An initial sulfide-saturated basaltic liquid should easily maintain sulfide saturation during fractional crystallization.

Application to ore genesis

Equation 9 can be used to monitor the SCSS during cooling and isobaric fractionation of a mafic magma. Of particular interest is the segregation of immiscible sulfide liquid that may have accompanied cooling of the impact melt sheet that gave rise to the Sudbury Igneous Complex and its associated Ni-sulfide mineralization. Keays and Lightfoot (2004) have recently presented a model based in part on the enhanced solubility of S in high-temperature magmas. Lightfoot et al. (2001) estimated that the composition of the impact-generated melt sheet was that of a quartz diorite with ~60 wt% SiO_2, 7.5 wt% FeO, and 500 ppm S (Table 5). Ivanov and Deutsch (1997) have estimated that the impact sheet was

Table 5 Compositions and calculated liquidus temperatures of selected magmas

Parental melt	SiO_2	TiO_2	Al_2O_3	Cr_2O_3	FeO^{total}	MnO	MgO	CaO	Na_2O	K_2O	T°C
MORB[a]	49.61	0.83	16.04		9.24		9.89	11.68	2.32	0.03	1240
Basaltic andesite[b]	55.87	0.37	12.55	0.14	9.15	0.21	12.65	7.29	1.53	0.77	1336
B_3magma[c]	50.70	0.41	16.03	0.03	9.14	0.17	9.21	11.14	2.52	0.23	1241
SIC[d]	60.00	0.89	15.50		7.47	0.13	4.30	6.10	2.70	1.90	1188
SLI[e]	47.60	2.28	14.00		12.82		8.30	9.40	2.47	0.55	1225
Ol tholeiite[f]	49.50	0.80	18.20		8.40	0.13	8.80	11.40	2.38	0.19	1245
Minimum melt[g]	75.89	0.28	12.99		1.46		0.31	1.02	3.11	4.85	1039

[a]Mid-ocean ridge basalt: sample K-17-20 from Galapagos 95.5°W (Wallace and Carmichael 1992), anhydrous, QFM, 1 kbar.
[b]Chill phase of the Lower Zone of the Bushveld Complex (Harmer and Sharpe 1985), 1 wt% H_2O, QFM, 2 kbar.
[c]Chill phase of the Main Zone of the Bushveld Complex (Sharpe 1981), QFM, 2 kbar.
[d]Average compositions of 49 marginal zone samples from the Worthington offset Sudbury Igneous Complex (SIC) (Lightfoot et al. 2001), anhydrous, QFM, 1 kbar.
[e]Bulk composition of the Sonju Lake Intrusion (SLI) (Miller and Ripley 1996), anhydrous, QFM, 2 kbar.
[f]Average composition of olivine tholeiite basalts from the Duluth area (Brannon 1984), anhydrous, QFM, 2 kbar.
[g]S-type minimum melt (White and Chappell 1977), anhydrous, QFM, 2 kbar

initially superheated, with a temperature of ~1,700°C. At a pressure of 1 kbar this melt would be capable of dissolving ~1,600 ppm S, and would therefore not be sulfide-saturated. On cooling, sulfide saturation would be reached at ~1,225°C; an immiscible sulfide liquid would separate and could accumulate by gravitational settling prior to the initiation of orthopyroxene crystallization at ~1,188°C (Fig. 8). Using a revised estimate of the S content of the combined felsic and mafic norites at Sudbury of 1,070 ppm (Keays and Lightfoot 2004), sulfide saturation may have been achieved at a temperature close to 1,500°C (Fig. 8). Dense immiscible sulfide liquid would be expected to accumulate near the base of the magma well before the silicate liquidus was reached,

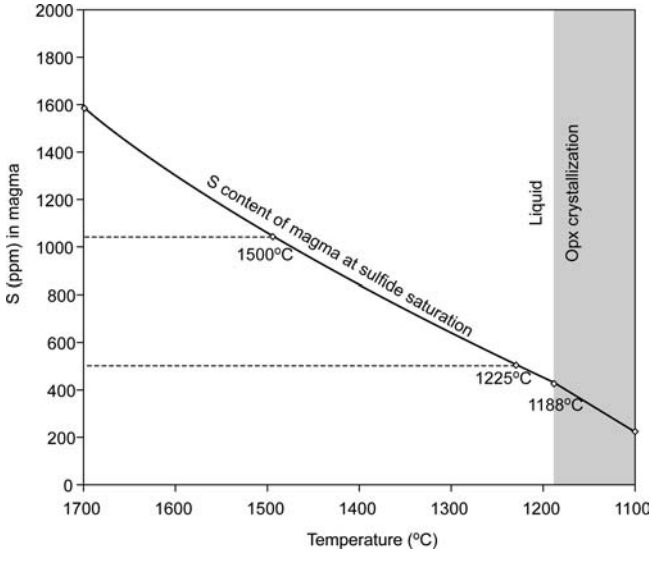

Fig. 8 Calculated SCSS with cooling of the Sudbury impact melt. The composition of the impact melt is taken from Lightfoot et al. (2001, Table 5). The silicate liquidus temperature is calculated for 1 kbar and fO_2 of QFM using MELTS (Ghiorso and Sack 1995). The SCSS has been calculated using Eq. 9. The values of 500 ppm S and 1,070 ppm S, are estimates of the S content of the bulk melt (Lightfoot et al. 2001) and a weighted average of felsic and mafic norite (Keays and Lightfoot 2004)

which is consistent with the observed geological relationships.

Other examples of applications of Eq. 9 in the area of ore genesis include the computation of sulfide saturation levels during mantle melting, fractional crystallization, and magma mixing. We have illustrated previously how Eq. 9 may be utilized to compute sulfide saturation levels during the fractional crystallization of a mafic magma. This may be an important process for reef-type PGE deposits where metal enrichment also occurs during the process. The Sonju Lake Intrusion (SLI) of the Duluth Complex, MN, provides an example of a relatively low-grade reef-type PGE occurrence. Enrichment in PGEs occurs at a well-defined interval in the layered sequence that comprises the SLI (Miller and Ripley 1996; Fig. 9). Miller and Andersen (2002) have referred to such enrichment in tholeiitic layered intrusions as the "Skaergaard" type, named after the PGE reefs that have been detected in the Skaergaard Intrusion. Miller (1999) has proposed that the PGE enrichment in the SLI is correlative with the attainment of sulfide saturation in the magma as a result of fractional crystallization. The magma that produced the SLI was relatively evolved with an initial FeO content of ~13 wt% (Table 5). Figure 10 illustrates the computed SCSS values during fractional crystallization of the parent magma using Zr as an index of crystallization. Our calculations indicate that sulfide saturation should be achieved when magnetite (or a Ti-bearing Fe-oxide such as titanomagnetite) joins plagioclase and clinopyroxene as a liquidus phase. The S content of the parent magma of the SLI is poorly constrained; for this reason we show several paths for S content during crystallization as a function of initial S concentration from ~300 ppm to 780 ppm. Our prediction of when sulfide saturation should have been achieved in the Sonju Lake magma matches field evidence which indicates that it was attained when titanomagnetite was a liquidus mineral at ~60% crystallization (within the oxide gabbro unit, Fig. 10).

The addition of S to a magma is a process that has been shown to be essential for many Ni–Cu–PGE

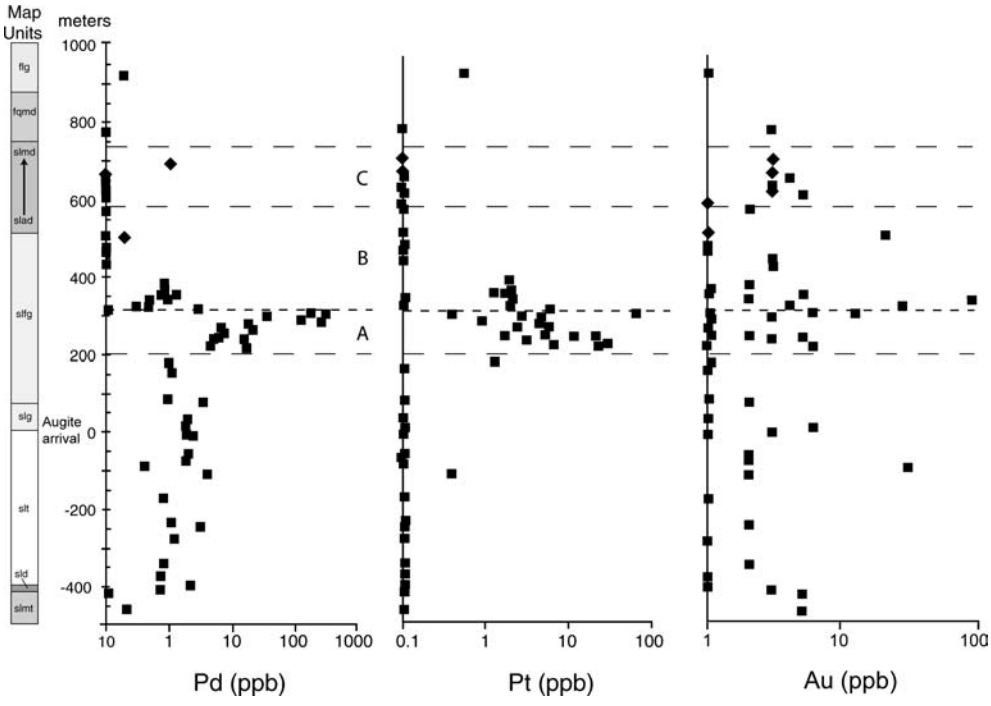

Fig. 9 Pd, Pt, and Au vs stratigraphic height in the Sonju Lake Intrusion (after Park et al. 2004). Miller (1999) has suggested that the peaks in the concentrations of Pt and Pd correspond to the attainment of sulfide saturation in the magma. This occurs after iron –titanium oxide has become a liquidus mineral. *sl* Sonju Lake Intrusion, *f* country rocks of the Finland Granophyre, *mt* melatroctolite, *d* dunite, *g* gabbro, *fg* oxide gabbro, *ad* apatite diorite, *md* monzodiorite, *gmd* quartz ferromonzodiorite, *g* micrographic granite

deposits, including Noril'sk (Grinenko 1985; Li et al. 2003b), Voisey's Bay (Ripley et al. 2002b), the Duluth Complex (Ripley 1981; Arcuri et al. 1998), and those associated with komatiites (Lesher and Keays 2002). The attainment of sulfide saturation in some magmas that host reef-type PGE deposits by the addition of S-bearing fluids to a magma has been proposed by Boudreau and Meurer (1999) and Willmore et al. (2000). The result of S addition to a magma in terms of sulfide saturation is readily evaluated by Eq. 9 and will not be considered further. However, contamination processes that involve mixing between a mafic magma and a Si-rich melt derived by partial melting of country rocks (magma silicification or felsification) has been proposed as a mechanism to induce sulfide saturation in the absence of any sulfur contributed by the country rocks (Irvine 1975; Li and Naldrett 1993; Lightfoot and Hawkesworth 1997). The estimation of the temperature of the contaminated magma is not an easy task, but in many cases (e.g., Ripley 1999) the oxygen isotopic compositions of coexisting minerals indicate not only that contamination has occurred, but also that equilibration occurred at temperatures in excess of 1,000°C. A possible implication of such observations is that mixing of the mafic magma and the melt derived from a country rock contaminant was complete before crystallization began.

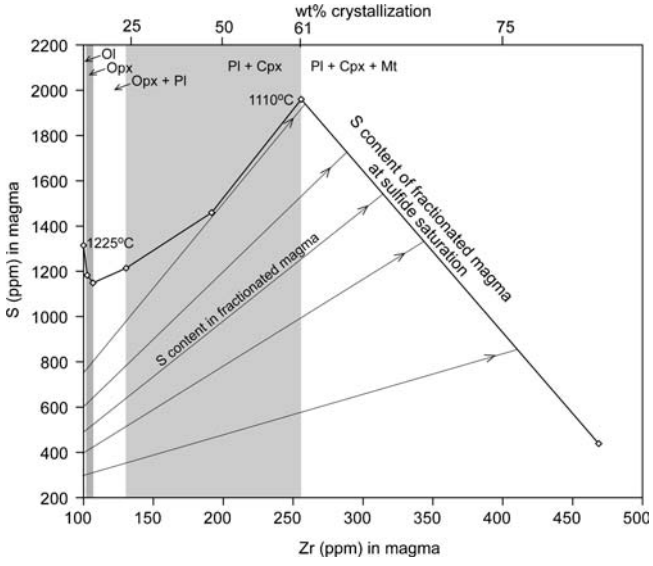

Fig. 10 The sulfur content at sulfide saturation vs Zr concentration for the estimated parent magma of the Sonju Lake Intrusion (Table 5, from Miller and Ripley 1996). The crystallization sequence was computed using MELTS (Ghiorso and Sack 1995) and the SCSS by Eq. 9. The S content in fractioned magma is shown for a variety of initial values. For any reasonable estimate of the initial S content of the Sonju Lake magma it is seen that sulfide saturation is reached after ~60% crystallization, when magnetite has joined plagioclase and clinopyroxene as a primocryst mineral. This prediction corresponds well to the observed peaks in Pt and Pd in the oxide gabbro unit of the Sonju Lake Intrusion, shown in Fig. 9

Figure 11illustrates mixing between an olivine tholeiite magma (a potential parental magma for many intrusions of the Duluth Complex; Miller and Ripley 1996) and a siliceous melt. The composition of the melt is similar to the "S-type" minimum melt of White and Chappell (1977) and to that produced by Hoffer and Grant (1980) in experimental studies of the partial melting of pelitic rocks (Table 5). These melt compositions were used by Ripley and Alawi (1988) to model partial melting of pelitic xenoliths by Duluth Complex magma. The diagram illustrates that the slopes of the

SCSS curve for the mixed magma at less than ~40% contamination are steeper than those of the lines for S concentration. At high degrees of mixing with a S-free contaminant, sulfide saturation will be induced. With contamination of ~10% and less this outcome is far less certain. Without consideration of the errors associated with the calculation of the SCSS, contamination of 10% and less may not cause the attainment of sulfide saturation. When the ±10% error of prediction is considered it is possible that even low degrees of mafic magma contamination by a siliceous, sulfur-poor melt could cause sulfide saturation. If the contaminant also contains sulfur then even very low amounts of contamination should lead to sulfide saturation.

The mixing of distinct mafic magmas represents a similar process to that described previously, but the composition of the "contaminant" is far less siliceous. Mixing of magmas is a process that has received considerable attention as a possible mechanism for initiating sulfide saturation in the mixed magma, and has been proposed as an integral process in the formation

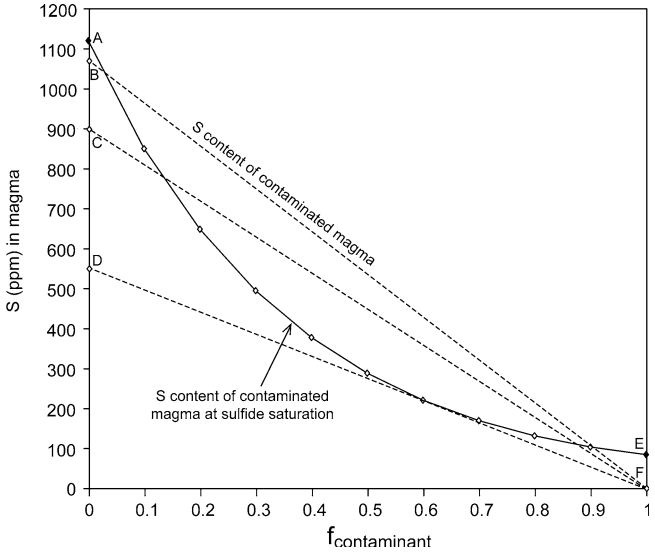

Fig. 11 Plot of the sulfur content of a contaminated mafic magma vs fractional abundance (*f*) of a S-free, Si-rich contaminant. The composition of the mafic melt is that of an olivine tholeiite (Brannon 1984), which is a potential parental magma for several intrusions of the Duluth Complex. The contaminant is taken as the "S-type" minimum melt of White and Chappell (1977), calculated on an anhydrous basis (Table 5). The liquidus temperatures of the mafic and silicic melts are 1,245 and 1,039°C. Partial melting of a pelitic rock with 2–4 wt% H_2O could lead to the production of a Si-rich melt at temperatures much lower than 1,038°C, but isotopic data often indicate that mixing occurred at elevated temperatures, prior to crystallization. The diagram indicates that sulfide saturation will be attained in the magma at high degrees of contamination, and may be unlikely at degrees of contamination less than ~5–10%. Points *A* and *E* are the sulfide saturation values for the end-members; points *B*, *C*, and *D* represent sulfur concentrations of three olivine tholeiite liquids; point *F* is the S concentration of the contaminant, taken as 0 ppm. Mixing of a siliceous melt and an olivine tholeiite will promote the attainment of sulfide saturation only if the mafic magma has a S concentration in excess of that represented by point *D*

of high-grade PGE deposits such as those of the Merensky Reef in the Bushveld Complex and the JM Reef in the Stillwater Complex (e.g., Campbell et al. 1983; Naldrett and von Gruenewaldt 1989). Li et al. (2001a) presented an equation to predict the sulfur content at sulfide saturation in a mafic magma, and utilized it to evaluate the role of magma mixing in the generation of sulfide and chromite mineralization in the Bushveld Complex. Cawthorn (2002) questioned the validity of the approach utilized by Li et al. (2001a), and based on phase equilibria and sulfur solubility constraints disputed the importance of magma mixing in producing a sulfide-saturated magma. There are three problems with the equation to predict the SCSS used by Li et al. (2001a): (1) the calibration was based on data collected from MORB only, and not on experimental results, (2) an incorrect assumption was made, namely that the SCSS was *linearly* related to temperature and FeO content of the magma, and (3) the temperature dependency of the equation was arbitrarily set. As long as the pressure, temperature, and composition of a magma produced in a mixing process can be established, Eq. 9 will permit the sulfide content at sulfide saturation over a relatively broad compositional range to be estimated. In Fig. 12a we show the SCSS of a basaltic andesite that is proposed by Barnes and Maier (2002) to be one of the magmas that produced the Merensky Reef of the Bushveld Complex (Table 5). Fractional crystallization of this magma will lead to sulfide saturation (e.g., path A–B) in a manner similar to that described above for the SLI. In our example, at ~30% crystallization when plagioclase becomes a liquidus mineral, a pulse of tholeiitic basalt (magma B_3), the second magma proposed by Barnes and Maier (2002) to be involved in the genesis of the Merensky Reef enters the chamber. Figure 12b illustrates the SCSS of several magma mixtures and indicates that if the basaltic magma which mixes with the remaining, fractionated, basaltic andesite contains in excess of ~800 ppm S, sulfide saturation will be maintained at low *f* (fractional abundance of tholeiitic basalt) values. Mixing of 67% of fractionated basaltic andesite (point C of Fig. 12a) with 33% of tholeiitic basalt containing ~920 ppm S (point C of Fig. 12b) will cause oversaturation of sulfide in the mixed magma. Mixtures with *f* values up to ~0.8 will be sulfide-oversaturated, with maximum oversaturation at a ratio of fractionated basaltic andesite to primitive tholeiitic basalt containing 920 ppm S of ~60/40. Sulfur that may be added to the mixed magma from the fluid being expelled from a crystallizing pile below the zone of mixing may add to the extent of oversaturation. Any compositional changes in the mixed magma brought upon by the incorporation of a S-bearing fluid would necessitate the computation of the SCSS for the appropriate magma composition.

We stress that any mixing model (two-component or multi-component) can only be as accurate as are the end-members that are utilized. The estimation of tem-

perature for a hybrid magma may also be difficult. Temperature is not an additive parameter, and even if crystallization is not induced by the mixing process, enthalpy data would be needed to estimate the temperature of the mixed magma. Figure 12b illustrates the need to compute the SCSS for the bulk composition of magma mixtures, as pointed out by Cawthorn (2002). Figure 12b also illustrates that if a mixed magma is sulfide-saturated or not is critically dependent on end-member compositions and mixing proportions, as well as pressure and temperature. For example, only small variations in the S content of an incoming magma may make a significant difference with respect to the mixed magma being sulfide undersaturated or oversaturated.

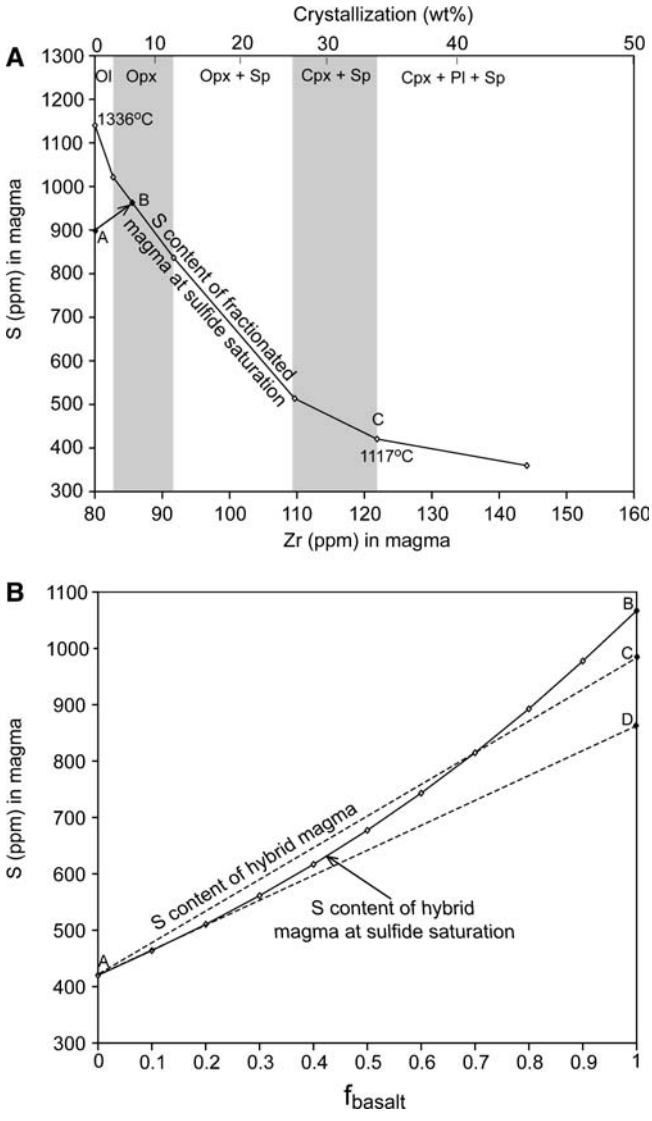

Fig. 12 **a** Sulfur content at sulfide saturation as a function of percent crystallization (Zr as an index) for a basaltic andesite thought to be involved in the formation of the Merensky Reef (Table 5). The crystallization sequence was determined using MELTS (Ghiorso and Sack 1995) at 2 kbar, QFM, and 1 wt% H_2O in the initial magma. Depending on the initial sulfur content of the magma, fractional crystallization (e.g., path *A*–*B*) may lead to rapid sulfide saturation. **b** The SCSS of hybrid magmas produced by mixtures of fractionated basaltic andesite (point *C* of **a**) and a tholeiitic basalt (magma B_3) proposed to be a second magma involved in the genesis of the Merensky Reef (Table 5). The fractional abundance of tholeiitic basalt in the mixture is f_{basalt}. The sulfur content of the mixed magma will lie on tielines between the sulfur content of the resident fractionated magma (here ~480 ppm) and the sulfur content of the added tholeiitic basalt. In this example a sulfur content of ~800 ppm (see point *D*) in the tholeiitic basalt would be required to maintain sulfide saturation in the mixed magma at low *f* values. If the sulfur content of the tholeiitic basalt were greater than 800 ppm, *f* values in excess of ~0.1 would lead to sulfide undersaturation in the mixed magma

Conclusions

Experimental data from Haughton et al. (1974), Danckwerth et al. (1979), Mavrogenes and O'Neill (1999), Holzheid and Grove (2002), O'Neill and Mavrogenes (2002), and Jugo et al. (2005) can be used to calibrate expressions for the prediction of the sulfide content of mafic magmas at the time of sulfide saturation. These empirical equations depend on temperature, pressure, and melt composition, and are strictly applicable to anhydrous mafic magmas at temperatures between 1,200 and 1,600°C and fO_2 conditions below QFM where sulfide is the predominant S species. The squared multiple correlation coefficients (r^2) for the regressions are greater than 0.88. Examples of processes which may be important for ore genesis, and to which the equations may be applied, include mantle and crustal melting, fractional crystallization, magma mixing, and contamination. Additional experimental studies are required to evaluate the systematics of S saturation in hydrous mafic magmas.

Acknowledgements Research at Indiana University on the genesis of magmatic sulfide-ore deposits has been supported by NSF Grants 9814204 to E.M. Ripley and 0104580 to C. Li and E.M. Ripley. Appreciation is expressed to Ed Mathez, Hugh O'Neill, Mike Lesher, John Mavrogenes, Rogerio Monteiro, and Tony Naldrett for reviews of an earlier draft of this manuscript.

Appendix

$$\text{predicted}X_S = \frac{\text{moles S}}{\text{moles magma} + \text{moles S}}$$

$$\text{moles S} = \frac{(X_S)(\text{moles magma from column}c)}{(1 - X_S)}$$

Using Eq. 9, the predicted ln X_S from this composition at a pressure of 1 bar and 1,200°C is −6.17, corresponding to $X_S = 0.002$, and 0.0032 mole of S. This equates to 0.1024 g of S or for a 100 g sample, 0.1024 wt%. Weight percent multiplied by 10,000 is ppm, therefore the predicted S content at sulfide saturation for this melt is 1,024 ppm.

Table 6 Example of calculations to convert oxide weight percents to mole fractions, and predict ppm S at sulfide saturation

	a	*b*	*c*	*d*	*e*
SiO_2	49.61	60.1	0.8254	0.5136	−0.67
TiO_2	0.83	79.9	0.0104	0.0065	−5.03
Al_2O_3	16.04	102.0	0.1572	0.0978	−2.32
Fe_2O_3	1.00	159.6	0.0063	0.0039	−5.55
FeO	8.35	71.8	0.1163	0.0724	−2.63
MgO	9.89	40.3	0.2454	0.1527	−1.88
CaO	11.68	56.1	0.2082	0.1296	−2.04
Na_2O	2.32	62.0	0.0374	0.0233	−3.76
K_2O	0.03	94.2	0.0003	0.0002	−8.52
Total (Σ)	99.75		1.6069	1.000	

a: wt% oxide $\left(\frac{\text{grams}}{100\,\text{g sample}}\right)$ for a mafic liquid

b: gram formula weight (molecular weight) of oxide

c: a/b = moles oxide

d: $c/\sum c$ = mole fraction

e: ln *d*.

References

Alt JC (1994) A sulfur isotopic profile through the Troodos ophiolite, Cyprus: primary composition and the effects of seawater hydrothermal alteration. Geochim Cosmochim Acta 58:1825–1840

Arcuri T, Ripley EM, Hauck SA (1998) Sulfur and oxygen isotope studies of the interaction between pelitic xenoliths and basaltic magma at the Babbitt and Serpentine Cu–Ni deposits, Duluth Complex, Minnesota. Econ Geol 93:1063–1075

Barnes S-J, Maier WD (2002) Platinum-group elements and microstructures of normal Merensky Reef from Impala Platinum Mine, Bushveld Complex. J Petrol 43:103–128

Boudreau AE, Meurer WP (1999) Chromatographic separations of the platinum-group elements, gold, base metals and sulfur during degassing of a compacting and solidifying crystal pile. Contrib Miner Petrol 134:174–185

Bradbury JW (1983) Pyrrhotite solubility in hydrous albite melts. PhD Thesis, The Pennsylvania State University, p 136

Brannon JC (1984) Geochemistry of successive lava flows of Keweenawan North Shore Volcanic Group. PhD Thesis, Washington University, St. Louis, p 212

Buchanan DL, Nolan J (1979) Solubility of sulfur and sulfide immiscibility in synthetic tholeiitic melts and their relevance to Bushveld-Complex rocks. Can Miner 17:483–494

Burnham CW (1979) Magmas and hydrothermal fluids. In: Barnes HL (ed) Geochemistry of hydrothermal ore deposits, 2nd edn. Wiley, New York, pp 71–136

Campbell IH, Naldrett AJ, Barnes SJ (1983) A model for the origin of the platinum-rich sulfide deposits in the Bushveld and Stillwater Complexes. J Petrol 24:133–165

Carroll MR, Rutherford MJ (1985) Sulfide and sulfate saturation in hydrous melts. Proceedings of the 15th Lunar Planetary Science Conference. J Geophys Res (Suppl) 90:C601–C612

Cawthorn RG (2002) The role of magma mixing in the genesis of PGE mineralization in the Bushveld Complex: thermodynamic calculations and new interpretations—a discussion. Econ Geol 97:663–666

Crockett JH (1979) Platinum-group elements in mafic-ultramafic rocks: a survey. Can Miner 17:391–402

Crockett JH (2002) Platinum-group element geochemistry of mafic and ultramafic rocks. In: Cabri LJ (ed) The geology, geochemistry, mineralogy and mineral beneficiation of platinum-group elements. Canadian Institute of Mining, Metallurgy, and Petroleum, Spe vol 54, pp 177–210

Danckwerth PA, Hess PC, Rutherford MJ (1979) The solubility of sulfur in high-TiO_2 mare basalts. Proceedings of the 10th Lunar Planetary Science Conference. Geochim Cosmochim Acta (Suppl) 517–530

Fincham CJB, Richardson FD (1954) The behaviour of sulphur in silicate and aluminate melts. Proc R Soc Lond Ser A 223:40–62

Gaetani GA, Grove TL (1997) Partitioning of moderately siderophile elements among olivine, silicate melt, and sulfide melt: constraints on core formation in the Earth and Mars. Geochim Cosmochim Acta 61:1829–1846

Ghiorso MS, Sack RO (1995) Chemical mass transfer in magmatic processes IV. A revised and internally consistent thermodynamic model for the interpolation and extrapolation of liquid–solid equilibria in magmatic systems at elevated temperatures and pressures. Contrib Miner Petrol 119: 197–212

Gorbachev NS, Kashiceva GA (1986) Fluid-magmatic differentiation of basaltic magma and equilibrium with magmatic sulfides. In: Experiments in the study of important problems in geology. Nauka, Moscow, pp 98–119

Green DH, Hibberson WD, Jaques AL (1979) Petrogenesis of mid-ocean ridge basalts. In: McElhinney MW (ed) The earth: its origin, structure, and evolution. Academic, San Diego, pp 265–299

Grinenko LN (1985) Sources of sulfur of the nickeliferrous and barren gabbro-dolerite intrusions of the northwest Siberian platform. Int Geol Rev 28:695–708

Harmer RE, Sharpe MR (1985) Field relations and strontium isotope systematics of the marginal rocks of the eastern Bushveld Complex. Econ Geol 80:813–837

Haughton DR, Roeder PL, Skinner BJ (1974) Solubility of sulfur in mafic magmas. Econ Geol 69:451–467

Helz RE (1977) Determination of the *P–T* dependence on the first appearance of FeS-rich liquid in natural basalts to 20 kb. EOS 58:523

Hess PC (1980) Polymerization model for silicate melts. In: Hargraves RP (ed) Physics of magmatic processes. Princeton University Press, New Jersey, pp 3–48

Hoffer E, Grant JA (1980) Experimental investigation of the formation of cordierite-orthopyroxene parageneses in pelitic rocks. Contrib Miner Petrol 73:15–22

Holzheid A, Grove TL (2002) Sulfur saturation limits in silicate melts and their implications for core formation scenarios for terrestrial planets. Am Miner 87:227–237

Huang W-L, Williams RJ (1980) Melting raltions of the system Fe–S–Si–O to 32 Kb with implications to the nature of the mantle-core boundary. Lunar Planet Sci Conf XI, Lunar Planet Sci Ins, pp 486–488

Irvine TN (1975) Crystallization sequences of the Muskox Intrusion and other layered intrusions: II. Origin of the chromitite layers and similar deposits of other magmatic ores. Geochim Cosmochim Acta 39:991–1020

Ivanov BA, Deutsch A (1997) Sudbury impact event: cratering mechanics and thermal history: large meteorite impacts and planetary evolution. Lunar Planet Inst Contrib 922:26

Jaupart C, Brandeis G (1986) The stagnant bottom layer of convecting magma chambers. Earth Planet Sci Lett 80:183–199

Jugo PJ, Luth RW, Richards JP (2005) An experimental study of the sulfur content in basaltic melts saturated with immiscible sulfide or sulfate liquids at 1,300°C and 1.0 GPa. J Petrol 46:783–798

Keays RR, Lightfoot PC (2004) Formation of Ni–Cu–platinum group element sulfide mineralization in the Sudbury impact melt sheet. Miner Petrol 82:217–258

Kress V (1997) Thermochemistry of sulfide liquids. I. The system O–S–Fe at 1 bar. Contrib Miner Petrol 127:176–186

Kress VC (2000) Thermochemistry of sulfide liquids II. Associated solution model for sulfide liquids in the system O–S–Fe. Contrib Miner Petrol 139:316–325

Langmuir CH, Klein EM, Plank T (1992) Petrological systematics of mid-ocean ridge basalts: constraints on melt genera-

tion beneath ocean ridges. In: Morgan JP, Blackman DK, Sinton JM (eds) Mantle flow and melt generation at mid-ocean ridges. Geophys Mon 71, Am Geophys Union, pp 183–280

Lesher CM, Keays RR (2002) Komatiite-associated Ni–Cu–(PGE) deposits: mineralogy, geochemistry, and genesis. In: Cabri LJ (ed) The geology, geochemistry, mineralogy, and mineral beneficiation of the platinum-group elements. Canadian Institute of Mining, Metallurgy, and Petroleum, Spe vol 54, pp 579–617

Lesher CM, Stone WE (1996) Exploration geochemistry of komatiites. In: Wyman D (ed) Igneous trace element geochemistry: applications for massive sulphide exploration. Geol Soc Can Short Course Notes, pp 153–204

Li J, Agee CB (1996) Geochemistry of mantle–core differentiation at high pressure. Nature 381:686–689

Li J, Agee CB (2001) The effect of pressure, temperature, oxygen fugacity and composition on partitioning of nickel and cobalt between liquid Fe–Ni–S alloy and liquid silicate: implications for the Earth's core formation. Geochim Cosmochim Acta 65:1821–1832

Li C, Naldrett AJ (1993) Sulfide capacity of magma: a quantitative model and its application to the formation of sulfide ores at Sudbury, Ontario. Econ Geol 88:1253–1260

Li C, Maier WD, de Waal SA (2001a) The role of magma mixing in the genesis of PGE mineralization in the Bushveld Complex: thermodynamic calculations and new interpretations. Econ Geol 96:653–662

Li C, Naldrett AJ, Ripley EM (2001b) Critical factors for the formation of a Ni–copper deposit in an evolved magmatic system: lessons from a comparison of the Pants Lake and Voisey's Bay sulfide occurrences in Labrador, Canada. Miner Deposita 36:75–92

Li C, Ripley EM, Mathez EA (2003a) The effect of S on the partitioning of Ni between olivine and silicate melt in MORB. Chem Geol 201:295–306

Li C, Ripley EM, Naldrett AJ (2003b) Compositional variations of olivine and sulfur isotopes in the Noril'sk and Talnakh intrusions, Siberia: implications for ore-forming processes in dynamic magma conduits. Econ Geol 98:69–86

Lightfoot PC, Hawkesworth CJ (1997) Flood basalts and magmatic Ni, Cu, and PGE sulphide mineralization: comparative geochemistry of the Noril'sk (Siberian Traps) and West Greenland sequences. In: Mahoney JJ, Coffin MF (eds) Large igneous provinces, vol 100. American Geophysical Union Monograph, pp 357–380

Lightfoot PC, Keays RR, Doherty W (2001) Chemical evolution and origin of nickel sulfide mineralization in the Sudbury Igneous Complex, Ontario Canada. Econ Geol 96:1855–1876

Marsh BD (2002) On bimodal differentiation by solidification front instability in basaltic magmas, part 1: basic mechanics. Geochim Cosmochim Acta 66:2211–2229

Mathez EA (1976) Sulfur solubility and magmatic sulfides in submarine basalt glass. J Geophys Res 81:4269–4276

Mavrogenes JA, O'Neill HSC (1999) The relative effects of pressure, temperature and oxygen fugacity on the solubility of sulfide in mafic magmas. Geochim Cosmochim Acta 63:1173–1180

McDonough WF, Sun S-S (1995) The composition of the earth. Chem Geol 120:223–253

Miller JD (1999) Geochemical evaluation of platinum group element (PGE) mineralization in the Sonju Lake Intrusion, Finland, Minnesota. Minn Geol Soc Inf Circ 44:31

Miller JD, Andersen JCO (2002) Attributes of Skergaard-type PGE deposits [abs]. In: Boudreau A (ed) 9th International Platinum Symposium, Billings Montana, Duke University, pp 305–308

Miller JD, Ripley EM (1996) Layered intrusions of the Duluth Complex, USA. In: Cawthorn RG (ed) Layered intrusions of the Duluth Complex, USA. Elsevier, Amsterdam, pp 257–301

Mysen BO, Popp RK (1980) Solubility of sulfur in $CaMgSi_2O_6$ and $NaAlSi_3O_8$ melts at high pressure and temperature with controlled fO_2 and fS_2. Am J Sci 280:78–92

Naldrett AJ (1999) World-class Ni–Cu–PGE deposits: key factors in their genesis. Miner Deposita 34:227–240

Naldrett AJ, von Gruenewaldt G (1989) Association of platinum-group elements with chromite in layered intrusions and ophiolite complexes. Econ Geol 84:180–187

O'Neill HSC, Mavrogenes JA (2002) The sulfide capacity and the sulfur content at sulfide saturation of silicate melts at 1400°C and 1 bar. J Petrol 43:1049–1087

Park Y-R, Ripley EM, Miller JD, Li C, Mariga J, Shafer P (2004) Stable isotopic constraints on fluid-rock interaction and Cu–PGE–S redistribution in the Sonju Lake Intrusion, Minnesota. Econ Geol 99:325–338

Peach CL, Mathez EA, Keays RR (1990) Sulfide melt-silicate melt distribution coefficients for nickel and iron and implications for the distribution of other chalcophile elements. Geochim Cosmochim Acta 54:3379–3389

Poulson SR, Ohmoto H (1990) An evaluation of the solubility of sulfide sulfur in silicate melts from experimental data and natural samples. Chem Geol 85:57–75

Prendergast MD, Keays RR (1989) Controls of platinum-group element mineralization and the origin of the PGE-rich Main Sulphide Zone in the Wedza Subchamber of the Great Dyke, Zimbabwe: implications for the genesis of and exploration for, stratiform PGE mineralization in layered intrusions. In: Prendergast MD, James MJ (eds) Magmatic sulphides—the Zimbabwe volume. London, Institution of Mining and Metallurgy, pp 21–42

Presnall DC, Gudfinnson GH, Walter MJ (2002) Generation of mid-ocean ridge basalts at pressures from 1 GPa to 7 GPa. Geochim Cosmochim Acta 66:2073–2090

Ripley EM (1981) Sulfur isotopic studies of the Dunka Road Cu–Ni deposit, Duluth Complex, Minnesota. Econ Geol 76:610–620

Ripley EM (1999) Systematics of sulphur and oxygen isotopes in mafic igneous rocks and related Cu–Ni–PGE mineralization. In: Keays RR, Lesher CM, Lightfoot PC, Farrow CEG (eds) Dynamic processes in magmatic ore deposits and their application to mineral exploration, vol 13. Geol Assoc Can Short Course Notes, pp 133–158

Ripley EM, Alawi JA (1988) Petrogenesis of pelitic xenoliths at the Babbitt Cu–Ni deposit, Duluth Complex, Minnesota, USA. Lithos 21:143–159

Ripley EM, Brophy JG, Li C (2002a) Copper solubility in a basaltic melt and sulfide liquid/silicate melt partition coefficients of Cu and Fe. Geochim Cosmochim Acta 66:2791–2800

Ripley EM, Li C, Shin D (2002b) Paragneiss assimilation in the genesis of magmatic Ni–Cu–Co sulfide mineralization at Voisey's Bay, Labrador: δ^{34} S, δ^{13} C, and Se/S evidence. Econ Geol 97:1307–1318

Sharpe MR (1981) The chronology of magma influxes to the Eastern compartment of the Bushveld Complex as exemplified by its marginal border groups. J Geol Soc Lond 13B:307–326

Shima H, Naldrett AJ (1995) Solubility of sulfur in ultramafic melt and the relevance of the system Fe–S–O. Econ Geol 70:960–967

Wallace P, Carmichael ISE (1992) Sulfur in basaltic magmas. Geochim Cosmochim Acta 56:1683–1874

Wendlandt RF (1982) Sulfide saturation of basalt and andesite melts at high pressures and temperatures. Am Miner 67:877–885

White AJR, Chappell BW (1977) Ultrametamorphism and granitoid genesis. Techtonophysics 43:7–22

Willmore CC, Boudreau AE, Kruger FJ (2000) The halogen geochemistry of the Bushveld Complex, Republic of South Africa: implications for chalcophile element distribution in the Lower and Critical Zones. J Petrol 41:1517–1539